

Sloshing in vertical cylinders with circular walls: the effect of radial baffles

Nikolay Kuznetsov, Oleg Motygin

Abstract The behaviour of sloshing eigenvalues and eigenfunctions is studied for vertical cylindrical containers that have circular walls and constant (possibly infinite) depth. The effect of breaking the axial symmetry due to the presence of radial baffles is analysed. It occurs that the lowest eigenvalues are substantially smaller for containers with baffles going throughout the depth; moreover, all eigenvalues are simple in this case. On the other hand, the lowest eigenvalue has multiplicity two in the absence of baffle. It is shown how these properties affect the location of maxima and minima of the free surface elevation and the location of its nodes.

1 Introduction

The sloshing of a fluid in various partially filled containers is a topic of great interest to engineers, physicists and mathematicians. It has received extensive study; see, for example, the monographs [1] and [2] (the second one has more than 100 pages of references). A historical review going back to the 18th century can be found in [3], whereas the comprehensive book [4] presents an advanced mathematical approach to the problem based on spectral theory of operators in a Hilbert space. It is also worth mentioning that the 2012 Ig Nobel Prize for Fluid Dynamics was awarded to Krechetnikov and Mayer for their work [5] concerning the dynamics of sloshing when walking with a mug of coffee.

N. Kuznetsov

Laboratory for Mathematical Modelling of Wave Phenomena, Institute for Problems in Mechanical Engineering, Russian Academy of Sciences, V.O., Bol'shoy pr. 61, St. Petersburg 199178, Russian Federation e-mail: nikolay.g.kuznetsov@gmail.com

O. Motygin

Laboratory for Mathematical Modelling of Wave Phenomena, Institute for Problems in Mechanical Engineering, Russian Academy of Sciences, V.O., Bol'shoy pr. 61, St. Petersburg 199178, Russian Federation e-mail: mov@ipme.ru, o.v.motygin@gmail.com

The standard approach to sloshing is based on the linear water wave theory (see again the books [1] and [2]). In its framework, one seeks sloshing modes and frequencies using eigenfunctions and eigenvalues, respectively, of a mixed Steklov problem for the Laplace equation, and so a spectral parameter, say ν , appears in a boundary condition, whereas the radian frequency of fluid's oscillations is proportional to the square root of ν .

The question of suppression of sloshing by means of baffles (it is of importance for practice) goes back to the 1960s. The corresponding experimental and theoretical results were the topic of numerous NASA Technical Reports cited in [2] (in particular, a lot of data is summarised in [6]). In many cases, it was found that the effect of a baffle is to lower sloshing frequencies, especially, the lowest one. Therefore, a lot of research has been carried out in this field since the 1960s. In particular, some quite sophisticated techniques were developed for numerical evaluation of this effect during the past 30 years; here we mention a few methods that look the most interesting. In [7], eigenfunction expansions were applied on either side of a vertical baffle in a rectangular tank. By matching these expansions one obtains an integral equation on the interval below or above the baffle. The approach developed in [8], uses fundamental solutions of the problem for reducing it to an integral equation in the case of a vertical circular container with a horizontal annular baffle. The method of successive conformal mappings leading to standard truncated matrix eigenvalue problems which are then solved numerically was used in [9], where several different baffles in a horizontal circular cylinder were considered.

Despite abundant numerical and analytical results (see e.g. [10] and references therein), the mechanism of the baffle effect is far from being completely understood. The aim of this note is to show the crucial role of breaking the axial symmetry in this phenomenon. For this purpose we compare properties of explicit solutions obtained by separation of variables for two pairs of vertical cylindrical containers.

First, we consider sloshing frequencies and the corresponding modes that describe free oscillations of a fluid in a circular container of constant depth which has or has not the following radial baffle. It is located between the cylinder's axis and the vertical wall and goes throughout the container's depth. (According to Fox and Kuttler [3], it was Lord Rayleigh [11] who completed the solution of the problem without baffle, studies of which were initiated by Ostrogradsky and Poisson in the 1820s.) The second pair of containers includes the vertical annular cylinder without and with the radial baffle that connects the cylinder's walls orthogonally to them and goes throughout the container's depth. To the author's knowledge, no comparison of the described solutions was ever published. Thus, a gap concerning the mechanism of the hydrodynamic effect due to radial baffles is filled in at least partially.

2 Statement of the problem

The general formulation of the three-dimensional sloshing problem is as follows. A fluid domain, say W , is bounded from above by a free surface and from below

(and/or laterally) by the wetted rigid part of the container's boundary. The horizontal mean position of the free surface is a bounded two-dimensional domain, say F , that can be multiply connected, whereas $\partial W \setminus F$ is a piecewise-smooth surface whose boundary coincides with ∂F . Let Cartesian coordinates (x, y, z) be chosen so that the z -axis points upwards, the domain F belongs to the plane $z = 0$ and the rest part of ∂W lies in the half-space $z < 0$.

The usual hydrodynamic assumptions are as follows: the surface tension is neglected on the free surface; the fluid is inviscid, incompressible and heavy; its motion is irrotational and of small amplitude. Then sloshing modes and frequencies are sought using eigenfunctions and eigenvalues, respectively, of the following mixed Steklov problem (see [1–4]):

$$\nabla^2 \phi = 0 \quad \text{in } W, \quad (1)$$

$$\phi_z = \nu \phi \quad \text{on } F, \quad (2)$$

$$\frac{\partial \phi}{\partial n} = 0 \quad \text{on } \partial W \setminus \bar{F}, \quad (3)$$

$$\int_F \phi \, dx dy = 0. \quad (4)$$

Here ν is the spectral parameter and the last condition is imposed to exclude the eigenfunction identically equal to a non-zero constant that corresponds to the zero eigenvalue existing when the problem includes only relations (1)–(3).

In terms of (ν, ϕ) found from problem (1)–(4), the velocity field of free oscillations of the fluid occupying W is given by, say $\cos(\omega t + \alpha) \nabla \phi(x, y, z)$, where α is a certain constant, t stands for the time variable and $\omega = \sqrt{\nu g}$ is the radian frequency of oscillations (as usual, g denotes the acceleration due to gravity). Furthermore, the elevation of the free surface is proportional to $\sin(\omega t + \alpha) \phi(x, y, 0)$.

It is known that problem (1)–(4) has a sequence of eigenvalues (see, for example, [4] and [12]):

$$0 < \nu_1 \leq \nu_2 \leq \dots \nu_n \leq \dots, \quad \nu_n \rightarrow \infty,$$

to each of which a single eigenfunction ϕ_n corresponds, but if the multiplicity of an eigenvalue is greater than one (however, it always is finite), then this eigenvalue is repeated in the sequence as many times as the multiplicity is. Every ϕ_n belongs to the Sobolev space $H^1(W)$ (this means that both the kinetic and potential energy of the fluid motion are finite), whereas the set of these functions restricted to F forms together with a non-zero constant a complete orthogonal system in $L^2(F)$. It should be emphasised that the most important eigenfunction is ϕ_1 because it has the least rate of decay with time caused by non-ideal effects in real-life fluids.

3 Vertical circular containers without and with a radial baffle

In what follows, we use non-dimensional variables chosen so that the container's radius and the constant acceleration due to gravity are scaled to unity. For this purpose lengths are scaled to R , whereas the velocity potential ϕ is scaled to $(R^3 g)^{1/2}$ (nevertheless, we keep the same notation ϕ below); here R and g are the dimensional quantities for the container's radius and the gravity acceleration respectively. Furthermore, the non-dimensional spectral parameter is $\nu = R \omega^2 / g$ in this case.

3.1 Vertical circular container without baffle

In the non-dimensional variables introduced above, the fluid domain under consideration is $W = \{(x, y, z) : x^2 + y^2 < 1, z \in (-h, 0)\}$, where $h \in (0, \infty]$ (note that the case of infinite depth will be also considered). Thus we have that $F = \{(x, y, 0) : x^2 + y^2 < 1\}$ and $\partial W \setminus \bar{F} = \bar{B} \cup S$, where

$$B = \{(x, y, -h) : x^2 + y^2 < 1\} \quad \text{and} \quad S = \{(x, y, z) : x^2 + y^2 = 1, z \in (-h, 0)\}$$

are the bottom and the lateral cylindrical surface respectively. Therefore, it is natural to split the boundary condition (3) as follows:

$$\phi_r = 0 \quad \text{on } S, \quad \phi_z = 0 \quad \text{on } B. \quad (5)$$

Here and below r is the first component of the cylindrical coordinates (r, θ, z) such that $x = r \cos \theta$ and $y = r \sin \theta$.

The boundary conditions (5) allow us to separate the vertical coordinate, thus obtaining the following representations for the velocity potential and the spectral parameter respectively:

$$\phi(r, \theta, z) = u(r, \theta) \cosh k(z + h) \quad \text{and} \quad \nu = k \tanh kh. \quad (6)$$

It is clear from the last formula that ν is an increasing function of k . Moreover, ν increases with h , and so we have

$$\phi(r, \theta, z) = u(r, \theta) e^{kz} \quad \text{and} \quad \nu = k \quad \text{when } h = \infty. \quad (7)$$

Here, as well as in (6), u and k^2 must be found from the spectral problem

$$u_{xx} + u_{yy} + k^2 u = 0 \quad \text{in } F, \quad u_r(1, \theta) = 0 \quad \text{for } \theta \in [0, 2\pi], \quad \int_F u r \, dr d\theta = 0. \quad (8)$$

It is well known (see, for example, [13], § 3.2) that the set of eigenvalues of this problem can be written as the following infinite matrix:

$$(k_{m,s}^2)_{m=0,s=1}^\infty, \quad (9)$$

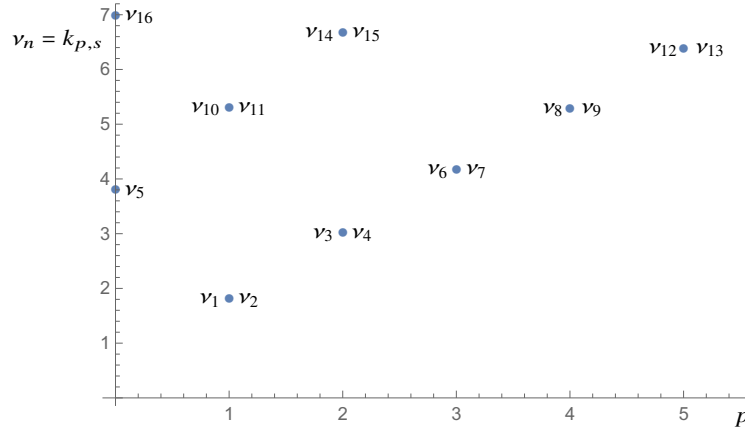


Fig. 1 Values v_n , $n = 1, 2, \dots, 16$ in the case of infinite depth.

where $k_{m,s}$ is the s th positive zero of J'_m — the derivative of the Bessel function J_m (for $m = 0$ this numbering differs from that used in [14], where $j'_{0,s}$ is the s th non-negative zero). Moreover, all eigenvalues are of multiplicity two when $m \neq 0$; in particular, the lowest eigenvalue is of multiplicity two as well as the other six corresponding to the eight initial zeroes of J'_m with various m , which are as follows in the increasing order:

$$\begin{aligned} k_{1,1} = 1.8411\dots, \quad k_{2,1} = 3.0542\dots, \quad k_{0,1} = 3.8317\dots, \quad k_{3,1} = 4.2011\dots, \\ k_{4,1} = 5.3175\dots, \quad k_{1,2} = 5.3314\dots, \quad k_{5,1} = 6.4156\dots, \quad k_{2,2} = 6.7061\dots \end{aligned} \quad (10)$$

The second formula (7) yields that these values are v_1, \dots, v_{15} for the infinitely deep container and among them only $v_5 = k_{0,1}$ is simple, whereas the next simple eigenvalue is $v_{16} = k_{0,2} = 7.0155\dots$ (the subsequence of simple eigenvalues is rather sparse); see Fig. 1.

If h is finite, then we have by the second formula (6) that

$$v_{m,s} = k_{m,s} \tanh k_{m,s} h, \quad m = 0, 1, \dots, \quad s = 1, 2, \dots \quad (11)$$

In particular, when $h = 2$ (the container's depth is equal to its diameter) the lowest sloshing eigenvalue is

$$v_1 = k_{1,1} \tanh 2 k_{1,1} \approx 1.8387, \quad (12)$$

which is sufficiently close to the fundamental eigenvalue shown in Fig. 1. Thus the fundamental eigenvalue defined by (11) differs from that for infinite depth only for sufficiently small h .

The eigenfunctions of problem (8) corresponding to every $k_{m,s}^2$, $m = 0, 1, \dots$, $s = 1, 2, \dots$, are as follows:

$$u_{m,s,1}(r, \theta) = J_m(k_{m,s} r) \cos m\theta, \quad u_{m,s,2}(r, \theta) = J_m(k_{m,s} r) \sin m\theta, \quad (13)$$

where $m \neq 0$ for the functions of the second type. Thus, every eigenfunction can be written in the form:

$$u_{m,s}(r, \theta) = AJ_m(k_{m,s} r) \cos(m\theta - \beta). \quad (14)$$

Here A is an arbitrary non-zero real constant and β is a number from $[0, 2\pi)$ when $m \neq 0$, that is, (14) is a non-trivial linear combination of the two functions (13) in this case; if $m = 0$, then $\cos \beta \neq 0$ can be included into A .

From (6) and (7), it follows that the elevation of the free surface is proportional to $\sin(\omega t + \alpha) u(x, y)$. Hence the free surface elevation of every sloshing eigenfunction attains its maxima and minima at the same points of \bar{F} , where the corresponding function (14) does. Also, the location of nodes on the free surface is defined by the nodal lines of (14) in F .

Let us consider in detail the properties of $u_{1,1}(r, \theta) = AJ_1(k_{1,1} r) \cos(\theta - \beta)$, corresponding to the lowest eigenvalue $k_{1,1}^2$ and defining the free surface elevation for the fundamental sloshing mode. To be specific we assume that $A > 0$, in which case $u_{1,1}$ attains its maximum and minimum at $(1, \beta)$ and $(1, \pi + \beta)$ respectively, because $J_1(k_{1,1} r)$ monotonically increases on $(0, 1)$. Since $\beta \in [0, 2\pi)$ is arbitrary, the maximum can be attained at any point on ∂F , whereas the minimum is attained at the point symmetric to the point of maximum with respect to the origin. The single nodal line of $u_{1,1}$ is the diameter orthogonal to that connecting the points of maximum and minimum. It is worth mentioning that these points for the fundamental sloshing mode are referred to as ‘high spots’ for the reason discussed in [15, 16].

Let us turn to properties of the functions $u_{m,s}$ when either m or s is greater than one. First, for every $u_{m,1}$ all its m maxima and m minima belong to ∂F and the points, where maxima and minima are attained, are symmetric with respect to the origin; moreover, each of m nodal lines is a diameter of F . Second, every $u_{1,s}$ has a single maximum and a single minimum inside the disc bounded by the innermost circular nodal line; the total number of nodal lines is s , one of which is a diameter of F , whereas the rest are circular. Finally, if both m and s are greater than one, then $u_{m,s}$ has maxima and minima on ∂F as well as inside F and nodal lines of both types (diameters and circles) exist.

The set of simple eigenvalues of problem (8) is $\{k_{0,s}^2\}_{s=1}^{\infty}$, and the axisymmetric eigenfunction $u_{0,s}(r, \theta) = AJ_m(k_{0,s} r)$ with $A \neq 0$ corresponds to each of these eigenvalues. If $A > 0$, then the global maximum is attained at the origin and the global minimum is attained at every point of the circumference $r = k_{0,1}/k_{0,s}$, whereas the points of ∂F deliver a negative (positive) local minimum (maximum respectively) when $s > 1$ is odd (even respectively). The eigenfunction $u_{0,s}$ has s nodal lines whose equations are $r = j_{0,n}/k_{0,s}$, $n = 1, \dots, s$, and $j_{0,n}$ is the n th positive zero of J_0 .

In particular, the eigenfunction $u_{0,1}(r, \theta) = AJ_m(k_{0,1} r)$ (it corresponds to the smallest simple eigenvalue for which $k_{0,1} = 3.8317\dots$) monotonically decreases with r and the equation of its single nodal line is $r = j_{0,1}/k_{0,1} \approx 0.6276$, where $j_{0,1} = 2.4048\dots$ is the least positive zero of J_0 .

3.2 Vertical circular container with a radial baffle

We assume that the second container is the same as above, but complemented by the rectangular rigid baffle $L = \{(r, 0, z) : r \in [0, 1], z \in [-h, 0]\}$, that is, the fluid domain is as follows:

$$\bar{W} = \{(r, \theta, z) : r \in (0, 1), \theta \in (0, 2\pi), z \in (-h, 0)\}.$$

Thus, $\partial\bar{W}$ — the boundary of the fluid domain — is the following union of surfaces $\bar{F} \cup L \cup \bar{B} \cup \bar{S}$. Here, the free surface \bar{F} and the container's bottom \bar{B} are F and B , respectively, from § 2.1 cut by the top and bottom side of L respectively, whereas the lateral cylindrical surface \bar{S} is S from § 2.1 cut vertically along the interval $\{r = 1, \theta = 0, z \in (-h, 0)\}$. Here and below the accent $\bar{}$ is used to distinguish notations from those for the container without baffle.

On both sides of L , the no-flow condition must hold, that is, the equalities

$$\phi_\theta(r, 0, z) = \phi_\theta(r, 2\pi, z) = 0 \quad \text{for } r \in (0, 1), z \in (-h, 0) \quad (15)$$

complement the boundary conditions (2) and (5).

Representations (6) and (7) are still valid because they depend only on the fact that the bottom is horizontal and on its depth. However, taking into account the boundary conditions (15), instead of (8), we obtain the spectral problem

$$u_{xx} + u_{yy} + k^2 = 0 \quad \text{in } \bar{F}, \quad u_r(1, \theta) = 0 \quad \text{for } \theta \in (0, 2\pi), \quad (16)$$

$$u_\theta(r, 0) = u_\theta(r, 2\pi) = 0 \quad \text{for } r \in (0, 1), \quad \int_{\bar{F}} ur \, dr d\theta = 0. \quad (17)$$

All eigenvalues of this problem are simple and they can be written in the matrix form similar to (9), but now the elements are equal to $\bar{k}_{m/2,s}^2$, $m = 0, 1, \dots$, $s = 1, 2, \dots$ (see [13], § 3.2). Here $\bar{k}_{p,s}$ is the s th positive zero of J'_p — the derivative of the Bessel function J_p with integer or half-integer $p \geq 0$ (again our notation differs from that in [14] for $m = 0$). The twenty initial values in the increasing order are as follows:

$$\begin{aligned} \bar{k}_{1/2,1} &= 1.1655\dots, \quad \bar{k}_{1,1} = 1.8411\dots, \quad \bar{k}_{3/2,1} = 2.4605\dots, \quad \bar{k}_{2,1} = 3.0542\dots, \\ \bar{k}_{5/2,1} &= 3.6327\dots, \quad \bar{k}_{0,1} = 3.8317\dots, \quad \bar{k}_{3,1} = 4.2011\dots, \quad \bar{k}_{1/2,2} = 4.6042\dots, \\ \bar{k}_{7/2,1} &= 4.7621\dots, \quad \bar{k}_{4,1} = 5.3175\dots, \quad \bar{k}_{1,2} = 5.3314\dots, \quad \bar{k}_{9/2,1} = 5.8684\dots, \\ \bar{k}_{3/2,2} &= 6.0292\dots, \quad \bar{k}_{5,1} = 6.4156\dots, \quad \bar{k}_{2,2} = 6.7061\dots, \quad \bar{k}_{11/2,1} = 6.9597\dots, \\ \bar{k}_{0,2} &= 7.0155\dots, \quad \bar{k}_{5/2,2} = 7.3670\dots, \quad \bar{k}_{6,1} = 7.5012\dots, \quad \bar{k}_{1/2,3} = 7.7898\dots \end{aligned} \quad (18)$$

It should be noted that $k_{1,1}$ — the first value in (10) — coincides with $\bar{k}_{1,1}$ which is second here, whereas the eighth value in (10) is only fifteenth here. It is clear that every eigenvalue $\bar{k}_{m/2,s}^2$ with even m is also an eigenvalue of problem (8), but for eigenvalues with odd m this is not true.

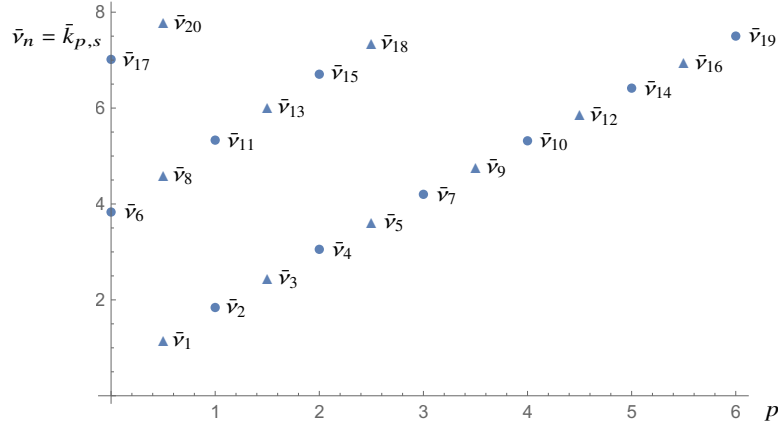


Fig. 2 Values $\bar{\nu}_n$, $n = 1, 2, \dots, 20$, for a circular container with baffle in the case of infinite depth.

As in § 2.1, the second formula (7) yields that the numbers (18) are the eigenvalues $\bar{\nu}_1, \dots, \bar{\nu}_{20}$ (shown in Fig. 2) for the infinitely deep container with a radial baffle. In this case, the ratios $\nu_1/\bar{\nu}_1, \dots, \nu_{16}/\bar{\nu}_{16}$ are as follows:

$$1.5796\dots, 1, 1.2412\dots, 1, 1.0547\dots, 1.0964\dots, 1, 1.1549\dots, \\ 1.1166\dots, 1.0026\dots, 1, 1.0932\dots, 1.0640\dots, 1.0452\dots, 1, 1.0080\dots$$

Since most of the eigenvalues have multiplicity two in the absence of baffle, we see that $\nu_n = \bar{\nu}_n$ for some n , but, in general, the behaviour of $\nu_n/\bar{\nu}_n$ demonstrates no regular pattern, at least for this initial part of the sequence.

If h is finite, then the second formula (6) gives that

$$\bar{\nu}_{m/2,s} = \bar{k}_{m/2,s} \tanh \bar{k}_{m/2,s} h, \quad m = 0, 1, \dots, s = 1, 2, \dots$$

To show how this formula distinguishes from (11) we take $h = 2$ —the same container's depth as in (12)—which gives for $m = 1$:

$$\bar{\nu}_1 = \bar{k}_{1/2,1} \tanh 2 \bar{k}_{1/2,1} \approx 1.1436.$$

Thus, $\bar{\nu}_1 \approx \nu_1 \cdot 0.6220$, and so the presence of the radial baffle in this circular container substantially diminishes the lowest sloshing eigenvalue comparing with the same container without baffle. Comparison of $\bar{k}_{p,s}$ and $\bar{\nu}_{p,s}$ for $h = 0.5$ is done in Fig. 3.

In view of conditions imposed on u_θ on both sides of the baffle, problem (16), (17) has only one eigensolution corresponding to the eigenvalue $\bar{k}_{m/2,s}^2$, namely

$$\bar{u}_{m,s}(r, \theta) = J_{m/2}(\bar{k}_{m/2,s} r) \cos \frac{m\theta}{2}, \quad m = 0, 1, 2, \dots, s = 1, 2, \dots \quad (19)$$

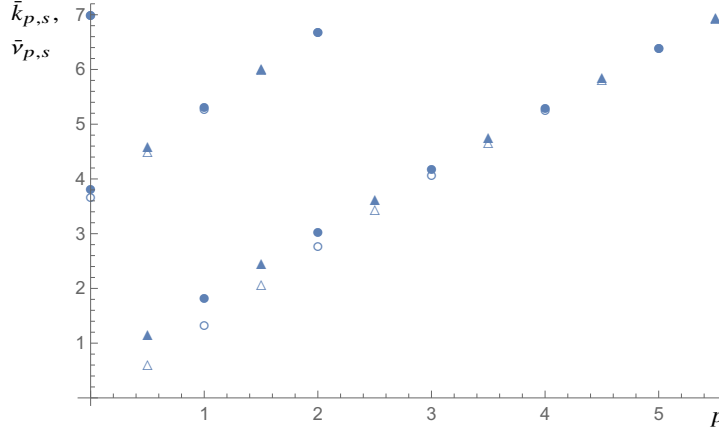


Fig. 3 Comparison of $k_{p,s}$ (disks), $\bar{k}_{p,s}$ (disks and filled triangles)—corresponding to the infinite depth case—and $k_{p,s} \tanh h k_{p,s}$ (circles), $\bar{k}_{p,s} \tanh h \bar{k}_{p,s}$ (circles and triangles) for the finite depth $h = 0.5$.

Its properties concerning maxima, minima and nodal lines are absolutely different from those of $u_{m,s}$; see formula (14). Let us consider these properties for the fundamental eigenfunction

$$\bar{u}_{1,1}(r, \theta) = J_{1/2}(\bar{k}_{1/2,s} r) \cos \frac{\theta}{2}.$$

It is an odd function of y , and so the unit interval of the negative x -axis is its nodal line. Furthermore, $\bar{u}_{1,1}(1, 0)$ and $\bar{u}_{1,1}(1, 2\pi)$ are the only maximum and minimum values of this function. The fact that the ‘high spots’ are the points $(1, 0)$ and $(1, 2\pi)$ adjacent to the baffle L is of practical importance because it is easier to suppress extremal sloshing localised at a particular place.

Turning to the case when either m or s is greater than one, we first consider $\bar{u}_{m,1}$ with $m \geq 2$. All m maxima and m minima of this function belong to

$$\{(r, \theta) : r = 1, \theta \in [0, 2\pi]\}.$$

Moreover, if m is odd, then $\bar{u}_{m,1}$ is an odd function of y , and $(1, 0)$ and $(1, 2\pi)$ are the points, where maximum and minimum, respectively, are attained by this function. Its other points of maxima and minima are also symmetric about the x -axis. All nodal lines of $\bar{u}_{m,1}$ with odd m are diameters of the unit disc with exception for the unit interval of the negative x -axis.

In the case of even m , formula (19) yields that $\bar{u}_{m,1}$ is an even function of y , and both $(1, 0)$ and $(1, 2\pi)$ are points of maximum for this function. Other points of maximum are also symmetric about the x -axis and the same is true for the points of minimum. All nodal lines of $\bar{u}_{m,1}$ with even m are diameters of the unit disc.

Properties of $\bar{u}_{1,s}$ with $s \geq 2$ and $\bar{u}_{m,s}$ when both m and s are greater than one are similar to those of $u_{1,s}$ with $s \geq 2$ and $u_{m,s}$ respectively.

As in § 2.1, every sloshing eigenfunction has maxima and minima of its free surface elevation at the same points of \bar{F} , where the corresponding function (19) does. Also, the location of nodes on the free surface is defined by the nodal lines of functions (19) in \bar{F} .

4 Vertical annular containers without and with a radial baffle

In this section, we use non-dimensional variables chosen so that the container's exterior radius and the constant acceleration due to gravity are scaled to unity (see § 2 for details).

4.1 Vertical annular container without baffle

Let ρ denote the non-dimensional radius of the inner wall coaxial with the exterior one, then the fluid domain under consideration is

$$W^\circ = \{(x, y, z) : \rho < x^2 + y^2 < 1, z \in (-h, 0)\}, \quad \text{where } h \in (0, \infty].$$

Representations (6) and (7) are valid because they depend only on the fact that the bottom is horizontal and on its depth. Taking into account the boundary conditions (15), we obtain the spectral problem

$$u_{xx} + u_{yy} + k^2 = 0 \quad \text{in } F^\circ = \{(x, y) : \rho < x^2 + y^2 < 1\}, \quad (20)$$

$$u_r(1, \theta) = u_r(\rho, \theta) = 0 \quad \text{for } \theta \in (0, 2\pi), \quad \int_{F^\circ} u_r \, dr d\theta = 0. \quad (21)$$

Using [13] we write the solutions to (20), (21) as follows:

$$u_{m,s}^\circ(r, \theta) = \frac{J_m(k_{m,s}^\circ r) Y_m'(k_{m,s}^\circ) - J_m'(k_{m,s}^\circ) Y_m(k_{m,s}^\circ r)}{J_m(k_{m,s}^\circ) Y_m'(k_{m,s}^\circ) - J_m'(k_{m,s}^\circ) Y_m(k_{m,s}^\circ)} \begin{cases} \cos m\theta, \\ \sin m\theta \quad (m \neq 0), \end{cases} \quad (22)$$

where $m = 0, 1, 2, \dots$, $J_m(\cdot)$ and $Y_m(\cdot)$ are Bessel's functions of the first and the second kind. The denominator in (22) is introduced to normalize the radial factor to unity at $r = 1$. The values $k_{m,s}^\circ$, for a fixed m and $s = 1, 2, 3, \dots$, are the increasing roots of the equation

$$J_m'(k_{m,s}^\circ) Y_m'(\rho k_{m,s}^\circ) - J_m'(\rho k_{m,s}^\circ) Y_m'(k_{m,s}^\circ) = 0. \quad (23)$$

For the properties of the cross-product in the left-hand side, see, e.g., [17, 18] and references therein.

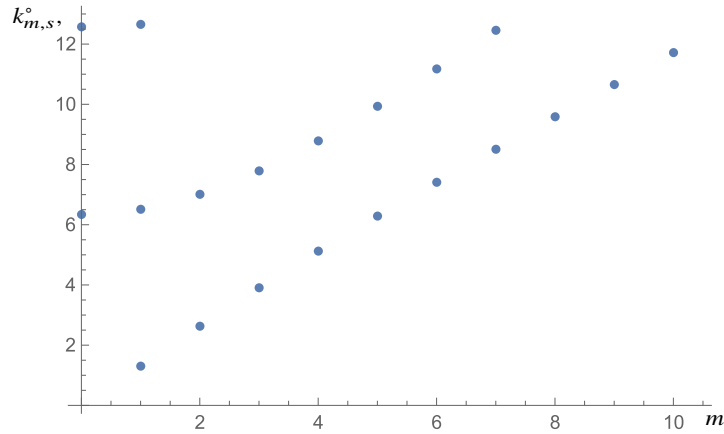


Fig. 4 Values $k_{m,s}^{\circ}$ for an annular container of infinite depth without baffle, $\rho = 1/2$.

A set of values $k_{m,s}^{\circ}$, computed for $\rho = 1/2$, is shown in Fig. 4 and is given here in the ascending order:

$$\begin{aligned}
 k_{1,1}^{\circ} &= 1.3546\dots, & k_{2,1}^{\circ} &= 2.6812\dots, & k_{3,1}^{\circ} &= 3.9577\dots, & k_{4,1}^{\circ} &= 5.1752\dots, \\
 k_{5,1}^{\circ} &= 6.3388\dots, & k_{0,1}^{\circ} &= 6.3931\dots, & k_{1,2}^{\circ} &= 6.5649\dots, & k_{2,2}^{\circ} &= 7.0625\dots, \\
 k_{6,1}^{\circ} &= 7.4621\dots, & k_{3,2}^{\circ} &= 7.8401\dots, & k_{7,1}^{\circ} &= 8.5586\dots, & k_{4,2}^{\circ} &= 8.8364\dots, \\
 k_{8,1}^{\circ} &= 9.6382\dots, & k_{5,2}^{\circ} &= 9.9858\dots, & k_{9,1}^{\circ} &= 10.7070\dots, & k_{6,2}^{\circ} &= 11.2269\dots, \\
 k_{10,1}^{\circ} &= 11.7688\dots, & k_{7,2}^{\circ} &= 12.5094\dots, & k_{0,2}^{\circ} &= 12.6246\dots, & k_{1,3}^{\circ} &= 12.7064\dots
 \end{aligned}$$

It should be noted at the point that all eigenvalues $[k_{m,s}^{\circ}]^2$ for $m, s = 1, 2, \dots$ have multiplicity two, whereas $[k_{0,s}^{\circ}]^2$ for $s = 1, 2, \dots$ are simple.

4.2 Vertical annular container with a radial baffle

In the section we assume that the container is the same as above, but complemented by the rectangular rigid baffle $L = \{(r, 0, z) : r \in [\rho, 1], z \in [-h, 0]\}$, that is, the fluid domain is as follows:

$$\bar{W}^{\circ} = \{(r, \theta, z) : r \in (\rho, 1), \theta \in (0, 2\pi), z \in (-h, 0)\}.$$

On both sides of L , the no-flow condition must hold, that is, the equalities

$$\phi_{\theta}(r, 0, z) = \phi_{\theta}(r, 2\pi, z) = 0 \text{ for } r \in (\rho, 1), z \in (-h, 0)$$

complement the boundary conditions.

Representations (6) and (7) are still valid. Taking into account the boundary conditions (15), we obtain the spectral problem

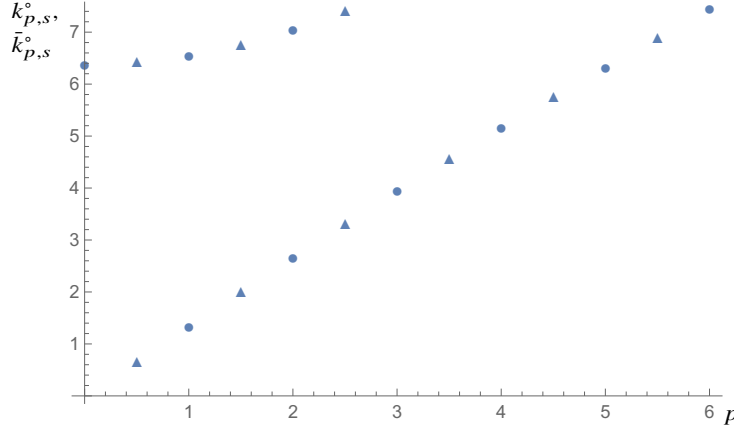


Fig. 5 Values $k_{p,s}^{\circ}$ (disks) for an annular container without baffle, $\rho = 1/2$, and values $\bar{k}_{p,s}^{\circ}$ (disks and filled triangles) for an annular container with baffle, $\rho = 1/2$.

$$u_{xx} + u_{yy} + k^2 = 0 \text{ in } \bar{F}^{\circ}, \quad u_r(1, \theta) = u_r(\rho, \theta) = 0 \text{ for } \theta \in (0, 2\pi), \quad (24)$$

$$u_{\theta}(r, 0) = u_{\theta}(r, 2\pi) = 0 \text{ for } r \in (\rho, 1), \quad \int_{\bar{F}^{\circ}} ur \, dr d\theta = 0. \quad (25)$$

All eigenvalues of this problem, namely, $[\bar{k}_{m/2,s}^{\circ}]^2$, $m = 0, 1, 2, \dots$, $s = 1, 2, \dots$, are simple; we can write the solutions to (24), (25) as follows:

$$\bar{u}_{m,s}^{\circ}(r, \theta) = R_{m/2,s}(r) \cos \frac{m}{2} \theta,$$

where $R_{m/2,s}(r) = \hat{R}_{m/2,s}(r) / \hat{R}_{m/2,s}(1)$ (normalized to 1 at $r = 1$),

$$\hat{R}_{m/2,s}(r) = J_{m/2}(\bar{k}_{m/2,s}^{\circ} r) Y'_{m/2}(\bar{k}_{m/2,s}^{\circ}) - J'_{m/2}(\bar{k}_{m/2,s}^{\circ}) Y_{m/2}(\bar{k}_{m/2,s}^{\circ} r),$$

$J_{m/2}(\cdot)$ and $Y_{m/2}(\cdot)$ are Bessel's functions of the first and the second kind. Here the values $\bar{k}_{m/2,s}^{\circ}$, for a fixed m and $s = 1, 2, 3, \dots$, are the increasing roots of the equation

$$J'_{m/2}(\bar{k}_{m/2,s}^{\circ}) Y'_{m/2}(\rho \bar{k}_{m/2,s}^{\circ}) - J'_{m/2}(\rho \bar{k}_{m/2,s}^{\circ}) Y'_{m/2}(\bar{k}_{m/2,s}^{\circ}) = 0. \quad (26)$$

Some initial values for $\rho = 1/2$ (see Fig. 5) in the increasing order are as follows:

$$\begin{aligned} \bar{k}_{1/2,1}^{\circ} &= 0.6791\dots, \quad \bar{k}_{1,1}^{\circ} = 1.3546\dots, \quad \bar{k}_{3/2,1}^{\circ} = 2.0230\dots, \quad \bar{k}_{2,1}^{\circ} = 2.6812\dots, \\ \bar{k}_{5/2,1}^{\circ} &= 3.3266\dots, \quad \bar{k}_{3,1}^{\circ} = 3.9577\dots, \quad \bar{k}_{7/2,1}^{\circ} = 4.5738\dots, \quad \bar{k}_{4,1}^{\circ} = 5.1752\dots, \\ \bar{k}_{9/2,1}^{\circ} &= 5.7630\dots, \quad \bar{k}_{5,1}^{\circ} = 6.3388\dots, \quad \bar{k}_{0,1}^{\circ} = 6.3931\dots, \quad \bar{k}_{1/2,2}^{\circ} = 6.4363\dots, \\ \bar{k}_{1,2}^{\circ} &= 6.5649\dots, \quad \bar{k}_{3/2,2}^{\circ} = 6.7754\dots, \quad \bar{k}_{11/2,1}^{\circ} = 6.9046\dots, \quad \bar{k}_{2,2}^{\circ} = 7.0625\dots, \\ \bar{k}_{5/2,2}^{\circ} &= 7.4199\dots, \quad \bar{k}_{6,1}^{\circ} = 7.4621\dots \end{aligned}$$

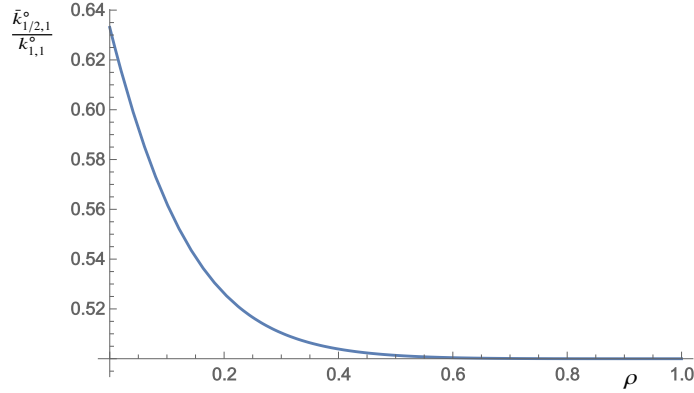


Fig. 6 Ratio $\bar{k}_{1/2,1}^\circ/k_{1,1}^\circ$ (corresponding to the lowest sloshing eigenvalues) for annular container with and without baffle. Dependence on the internal radius ρ .

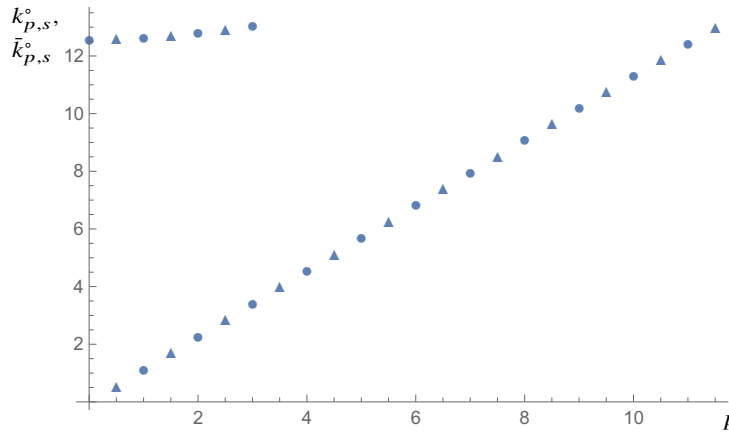


Fig. 7 Values $k_{p,s}^\circ$ (disks) for annular container without baffle, $\rho = 3/4$, and values $\bar{k}_{p,s}^\circ$ (disks and filled triangles) for annular container with baffle, $\rho = 3/4$.

It is important to note that the presence of the baffle in the annular container also substantially diminishes the lowest sloshing eigenvalue comparing with the same container without baffle. Figure 6 shows the dependence of the ratio $\bar{k}_{1/2,1}^\circ/k_{1,1}^\circ$ on the internal radius ρ . It can also be noted that the fundamental mode is expressed in a fairly simple form:

$$\bar{u}_{1,1}^\circ(r, \theta) = \frac{1}{\sqrt{r}} \left[\cos(\bar{k}_{1/2,1}^\circ(1-r)) - (2\bar{k}_{1/2,1}^\circ)^{-1} \sin(\bar{k}_{1/2,1}^\circ(1-r)) \right] \cos \frac{\theta}{2}.$$

Changes of $k_{m,s}^\circ$ and $\bar{k}_{m,s}^\circ$ as the annular container becomes thinner can be observed in Fig. 7, computed for $\rho = 3/4$. Using results of [19] and [20] on the asymptotic behaviour of the cross-product appearing in the left-hand side of (23)

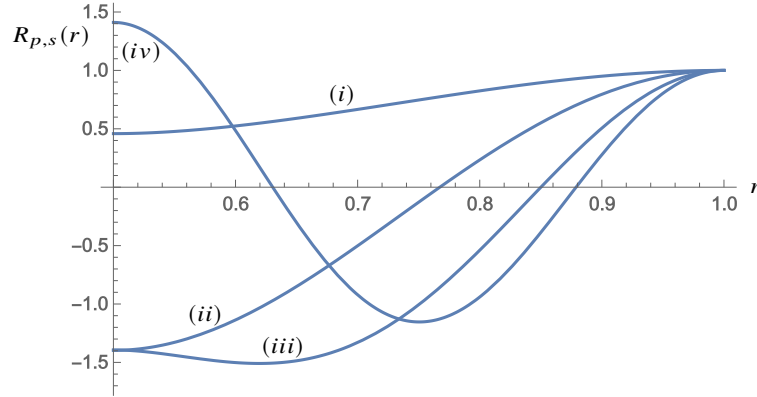


Fig. 8 Functions $R_{p,s}(r)$ for $\rho = 1/2$ and $\{p, s\} = \{4, 1\}$ (i), $\{p, s\} = \{0, 1\}$ (ii), $\{p, s\} = \{7, 2\}$ (iii), $\{p, s\} = \{1/2, 3\}$ (iv).

and (26), it can be shown that $\bar{k}_{p,1}^\circ \rightarrow p$ as $\rho \rightarrow 1^-$, whereas $\bar{k}_{p,s}^\circ \rightarrow \infty$ for $s = 2, 3, \dots$

Of interest is the position of extrema of the radial component of the eigenfunction $R_{m/2,s}(r)$ as $r \in [\rho, 1]$. In Fig. 8 some specific forms of $R_{m/2,s}(r)$ are presented for $\rho = 1/2$ to demonstrate different positions of the ‘high spots’. The curve (i) corresponds to $\bar{k}_{4,1}^\circ = 5.1752\dots$ and the maximum is located at the point, where the baffle is attached to the outer side wall ($r = 1$). The curve (ii) corresponds to $\bar{k}_{0,1}^\circ = 6.3931\dots$ and the minimum is located at the point, where the baffle is attached to the inner side wall ($r = \rho$). The curve (iii) corresponds to $\bar{k}_{7,2}^\circ = 12.5094\dots$ and shows the case when the maximum of absolute value is located at an inner point of the baffle. The curve (iv) corresponds to $\bar{k}_{1/2,3}^\circ = 12.6451\dots$ and shows more complicated behaviour of the computed eigenfunctions as s increases.

5 Discussion

In § 3, we analysed solutions of two spectral problems one of which describes sloshing in a vertical circular container of constant (possibly infinite) depth, whereas the container considered in the other problem apart from the same bottom and side wall has also the vertical baffle that goes from the free surface to the bottom and connects the container’s axis with the side wall. Unlike the first container, which has uncountably many vertical planes of symmetry going through the container’s axis, the second one has only one plane of symmetry in which the baffle lies. The effect of broken symmetry leads to the essential difference of properties of sloshing eigenvalues and eigenfunctions; the most important of which are the following.

First, all eigenvalues of the container with baffle are simple, whereas in the absence of baffle each eigenvalue has multiplicity two except for those corresponding

to axisymmetric eigenmodes. This fact has essential influence on properties of eigenfunctions discussed below. Second, it occurs that the lowest eigenvalue is substantially smaller in the presence of baffle comparing with the case when there is no baffle. Third, the set of eigenvalues of the container without baffle is a subset of the set existing when the baffle is present; the difference between the latter and former sets is an infinite set. The elements of both subsets are intermittent without any apparent pattern.

Comparing properties of eigenfunctions, we see that of two linearly independent eigenfunctions, corresponding to every eigenvalue in the case when there is no baffle, one is an even function of y , whereas the other is odd. Therefore, locations of maxima and minima of the corresponding free surface elevation and of its nodes can be chosen arbitrarily. This follows from the fact that there are uncountably many linear combinations of linearly independent eigenfunctions.

On the other hand, every eigenfunction, existing in the presence of baffle, is either odd or even function of y provided the baffle lies in the (x, z) -plane. This leads to the completely different behaviour of sloshing modes in this case. For example, the elevation of the free surface, corresponding to the fundamental sloshing mode, has its maximum and minimum attained at the points, where the baffle is attached to the side wall. This, along with the diminished lowest eigenvalue, is the most important effect that results from the symmetry breaking by the radial baffle.

In § 4, similar results were obtained for an annular container with and without baffle. It is natural that behaviour of eigenvalues and eigenfunctions is more complicated, in particular including dependence on an additional parameter of the problem (thickness of the annulus). However, observations of effects of broken symmetry — as the baffle is added — are very similar to the case of a circular container.

References

1. Faltinsen, O.M., Timokha, A.N.: *Sloshing*. Cambridge University Press, New York (2009)
2. Ibrahim, R.A.: *Liquid Sloshing Dynamics*. Cambridge University Press, New York (2005)
3. Fox, D.W., Kuttler, J.R.: Sloshing frequencies. *ZAMP*. **34**, 668–696 (1983)
4. Kopachevsky, N.D., Krein, S.G.: *Operator Approach to Linear Problems of Hydrodynamics*. Birkhäuser, Basel – Boston – Berlin (2001)
5. Mayer, H., Krechetnikov, R.: Walking with coffee: Why does it spill? *Phys. Rev. E*. **85**, Art. No. 046117(1–7) (2012)
6. Abramson, H.N.: *Slosh suppression*. Washington DC, NASA SP-8031 (1969)
7. Evans, D.V., McIver, P.: Resonant frequencies in a container with vertical baffles. *J. Fluid Mech.* **175**, 295–307 (1987)
8. Gavriluk, I., Lukovsky, I., Trotsenko, Yu., Timokha, A.: Sloshing in a vertical circular cylindrical tank with an annular baffle. Part 1. Linear fundamental solutions. *J. Eng. Math.* **54**, 71–88 (2006)
9. Hasheminejad, S.M., Mohammadi, M.M.: Effect of anti-slosh baffles on free liquid oscillations in partially filled horizontal circular tanks. *Ocean Engineering*. **38**, 49–62 (2011)
10. Choudhary, N., Bora, S.N.: Linear sloshing frequencies in the annular region of a circular cylindrical container in the presence of a rigid baffle. *Sādhanā*. **42**, 805–815 (2017)
11. Strutt, J.W. (Lord Rayleigh): On waves. *Phil. Mag. S. 5*. **1**(4), 257–259 (1876)

12. Moiseev, N.N.: Introduction to the theory of oscillations of liquid-containing bodies. *Adv. Appl. Mech.* **8**, 233–289 (1964)
13. Grebenkov, D.S., Nguyen, B.-T.: Geometrical structure of Laplacian eigenfunctions. *SIAM Review*. **55**, 601–667 (2013)
14. Abramowitz, M., Stegun, I.A.: *Handbook of mathematical functions*. US National Bureau of Standards, Washington DC (1964)
15. Kulczycki, T., Kuznetsov, N.: ‘High spots’ theorems for sloshing problems. *Bull. Lond. Math. Soc.* **41**, 495–505 (2009)
16. Kulczycki, T., Kuznetsov, N.: On the ‘high spots’ theorem for fundamental sloshing modes in a trough. *Proc. R. Soc. Lond. A.* **467**, 1491–1502 (2011)
17. Gottlieb, H.P.W.: On the exceptional zeros of cross-products of derivatives of spherical Bessel functions. *ZAMP.* **36**, 491–494 (1985)
18. Sorolla, E., Mosig, J.R., Mattes, M.: Algorithm to calculate a large number of roots of the cross-product of Bessel functions. *IEEE Trans. Antennas Propag.* **61**, 2180–2187 (2013)
19. McMahon, J.: On the roots of the Bessel and certain related functions. *Ann. of Math.* **9**, 23–40 (1894-95)
20. Buchholz, H.: Besondere Reihenentwicklungen für eine häufig vorkommende zweireihige Determinante mit Zylinderfunktionen und ihre Nullstellen. *Z. angew. Math. Mech.* **29**, 356–367 (1949)